Chem. Chem. Technol., 2025,
Vol. 20, No. 1, pp. 060–071

Chemistry

DEVELOPMENT OF HIGH-STRENGTH BIOACTIVE GLASS-CERAMIC MATERIALS FOR THE RECONSTRUCTION OF LONG BONE DEFECTS

Oksana Savvova[1], Olena Babich[1,✉], Oleksii Fesenko[1], Valentyna Maltseva[2], Serhii Firsov[1], Tetiana Shkolnikova[3]

[1] Department of Chemistry and Integrated Technologies, O.M. Beketov National University of Urban Economy in Kharkiv, 17 Chornoglazivska St., Kharkiv 61002, Ukraine

[2] Laboratory of Connective Tissue Morphology, Sytenko Institute of Spine and Joint Pathology, National Academy of Medical Sciences of Ukraine, 80 Hryhoriia Skovorody St., Kharkiv 61024, Ukraine

[3] Department of General and Inorganic Chemistry, National Technical University «Kharkiv Polytechnic Institute», 2 Kyrpychova St.,61002 Kharkiv, Ukraine

✉ *Olena.Babich@kname.edu.ua*

https:// doi.org 10.23939/chcht20.01.060

Abstract. The critical need for the restoration of the human musculoskeletal system, damaged due to osteoporosis, blast injuries, and congenital anomalies, has been identified. The needs of regenerative medicine aimed at the maximum possible restoration of the structure and functions of damaged tissues have been outlined. The necessity for the development of bioactive materials to substitute long bone defects through the creation of glass-ceramic materials with high biological activity and mechanical strength has been established.

High-strength glass-ceramic materials have been developed through rapid low-temperature thermal treatment. These materials are characterized by the presence of bioactive phases such as hydroxyapatite and lithium phosphate, spodumene, eucryptite, diopside, and lithium disilicate. They can withstand significant mechanical (compressive strength 550–650 MPa, bending strength 350–450 MPa, fracture toughness 4.5–6.1 MPa·m0.5) and thermal (CTE = (40.5–79.2)·10^{-7}°C^{-1}) loads and are promising candidates for use as substitutes for bone tissue in long bone elements.

Keywords: bioactive glass-ceramic materials, phase formation, hydroxyapatite, spodumene, mechanical and thermal properties.

1. Introduction

Preserving human health and ensuring its restoration are cornerstones of national gene pool recovery. Developing healthcare systems is critically important, especially under wartime conditions. The need to restore the human musculoskeletal system is acutely felt among both the elderly and working-age populations due to the decreased lifespan caused by osteoporosis. The World Health Organization stresses the urgency of treating and preventing this disease.[1,2] The osteoporosis issue is exacerbated by environmental problems, poor-quality food, and water. Over the past two decades, an accelerating trend has been observed during periods of armed conflict, marked by a growing proportion of fatalities resulting from explosions. According to forensic anthropologists and prosthetics specialists, blast trauma is characterized by a high prevalence of injuries to the limbs (22.8–91.2%) and face (19.6–40%) during combat, as well as frequent fractures of the lower extremities (19–74.3%).

Potential indicators of blast trauma include blast fractures in the sinus cavities caused by excessive explosion pressure, transverse fractures of the mandible, and rib fractures on the visceral surface.[3] The nature of blast injuries depends on the characteristics of the tissue exposed to the blast wave phenomenon.[4]

Modern research into "bone microarchitecture disruption" helps identify bone quality aspects such as clinical vertebral fractures, distal radius fractures, proximal femur fractures, or proximal humerus fractures.[5] The classification proposed by the authors[6] allows verification of all long bone defects in clinical practice, enabling the selection of optimal standardized treatment methods and improving treatment outcomes by selecting appropriate replacement technologies.

Successful approaches to long bone defect restoration began with the introduction of the Ilizarov

method.[7] The main methods for restoring critical bone defects of the tibia, as outlined in this section of the literature review, have their limitations – primarily the relatively small defect length (up to 6 cm). At present, several approaches to addressing long bone defects can be distinguished:

– The use of auto- and heteroplastic grafts for bone defect replacement;

– Reconstruction of defects by fibula transplantation;

– Development and use of artificial materials for defect reconstruction: biodegradable polymers,[8] bioactive ceramics, and glasses.[9]

The main limiting factor in the treatment of segmental defects of long bones (LBSD) of considerable length is the inability to provide the required amount of autologous bone grafts for implantation into the defect area, or the high risk of nonunion when allografts or synthetic materials such as tricalcium phosphate, bioceramics, and others are used. Additionally, the cost of synthetic materials and allografts can be prohibitively high, especially considering the limited scientific evidence supporting their effectiveness.

The need to replace LBSD arises from conditions such as congenital bone diseases, arthritis, osteomyelitis, nonunion, bone infections, bone exposure, trauma, and bone tumor resection. Future studies of biomaterials for LBSD reconstruction are mainly focused on artificial biomaterials and bone tissue engineering, which offer flexibility in material design and fabrication and can best meet the requirements for LBSD reconstruction.[10] Moreover, achieving the "ideal" LBSD reconstruction cannot rely on a single biomaterial type; rather, the combination of two or more materials appears to be the most promising option.

Currently, regenerative medicine aims to restore bone by maximally reconstructing the structure and functions of damaged tissues or organs through replacement of damaged structures and/or stimulation of the endogenous regenerative potential. The pressing need for rapid bone regeneration and reduction in blood loss and limb amputations is a top priority of regenerative medicine, particularly in emergency and crises such as military conflicts, natural disasters, and catastrophes. This task can be addressed by developing biocompatible composite materials – scaffolds based on bioactive inorganic materials combined with growth factors and natural polymers.[11]

Analytical Review

Today, research into obtaining tissue-engineered constructs for bone regeneration is rapidly advancing, with osteoconductive scaffold matrices playing a key role. These scaffolds are created from metals (titanium and titanium alloys),[12] polymers (natural: collagen,[3] hyaluronic acid, chitosan; synthetic: polylactic acid (PLLA), polyglycolic acid (PLGA), polycaprolactone (PCL)),[14] and their composites,[15] ceramics (bioinert: corundum, zirconium dioxide;[6] bioactive: hydroxyapatite, tricalcium phosphate,[16] calcium phosphate glasses and glass-ceramics).

In general, known bioinert materials are unable to form strong biochemical bonds with bone tissue. Specifically, metal alloys are heavy, capable of forming galvanic pairs, and may be toxic due to alloying elements. Natural polymers are chemically and mechanically unstable and exhibit low resorption rates. Synthetic polymers such as PLLA and PLGA have low mechanical properties. Ceramic materials are characterized by brittleness and low elasticity. The use of porous bioactive ceramics,[16,17] glasses, glass-ceramics,[18] and their composites, which exhibit exceptional bone substitution capabilities and high osteoconductive and osteoinductive potential, is limited by their poor mechanical properties. Currently, glass-composite osteoconductive matrices – mostly based on the well-known bioactive glasses 45S5 and S53P4[19] – remain mechanically weak. Among commercially available glass-ceramic materials – Bioverit, Ceravital (GC), and Cerabone A/W (GC) (Table 1) – only the latter can be considered a potential candidate for replacing segmental long bone defects.

Cerabone A/W glass-ceramic demonstrates particularly high biological activity, high mechanical strength (bending strength of 178 MPa and compressive strength of 1080 MPa) (Table 1), and can be processed into various shapes. Since 1983, this glass-ceramic material has been successfully used in spinal and hip surgeries in patients with major bone lesions and defects. However, despite CERABONE® A/W having the highest mechanical strength among all currently developed bioceramics, glass-ceramic scaffolds made from this composition still cannot be used under load-bearing conditions. Furthermore, issues arise regarding long-term bone integration and the slow degradation of this glass-ceramic. Slow degradation may lead to a reduction in effective pore size *in vivo* due to fibrous tissue ingrowth and nonspecific protein adsorption on the material's surface.[20] As a result, significant attention in future bioactive glass-ceramic development has been focused on accelerating the formation of an apatite-like layer on the material surface while maintaining mechanical properties. One such composition includes (mol. %): CaO 20–60, MgO 0–30, P_2O_5 0–10, SiO_2 29–60, CaF_2 0–5, and modifying oxides ΣNa_2O, K_2O, Ru_2O, Cs_2O, Fr_2O, SrO, Bi_2O_3, ZnO, Ag_2O, B_2O_3, Cu_2O, MnO_2, Fe_2O_3, TiO_2 in the range of 0–10. This material can form a hydroxyapatite

layer in simulated body fluid (SBF) within one hour[21] and is produced by sintering at temperatures up to 800°C without holding time. The crystalline phase content of sintered samples ranged from 0 to 30 mass %, with diopside $CaMg(Si_2O_6)$ as the main crystalline phase and fluorapatite as a secondary phase. The resulting compact glasses showed bend strengths of 80–150 MPa and featured controllable biodegradation rates and bactericidal activity. However, due to the high chemical resistance of the crystalline phases present in the composition, the resorption periods will be prolonged, which may negatively affect the bone mineralization process. The relatively high melting (1590°C) and sintering (800–850°C) temperatures complicate the production process and increase the material cost.

The authors of this study previously developed bioactive composite materials with high mechanical properties (H = 5900–7820 MPa, K_{IC} = 1.48–2.22 MPa·$m^{1/2}$, HV = 3800–6200 MPa) (Table 1), suitable for use as implants in statically and dynamically loaded bone areas in maxillofacial surgery.[22,23]

Building on prior research, the authors developed a reinforced bioactive calcium phosphate silicate glass-ceramic material for bone replacement in load-bearing areas. The material consists of a frit containing Na_2O, K_2O, Li_2O, CaO, MgO, P_2O_5, B_2O_3, SiO_2, ZnO, TiO_2, MnO_2, Cu_2O, SrO, CaF_2, and according to the invention, additionally includes oxides of aluminum, zirconium, cerium, cobalt, vanadium, lanthanum, and molybdenum, with the following mass percentages: SiO_2 47.0–50.0; Al_2O_3 2.0–3.0; Li_2O 2.0–4.5; Na_2O 3.5–6.0; K_2O 4; ZrO_2 0.5–1.0; P_2O_5 9.0–10.0; CaO 15–17; ZnO 1.0–3.0; B_2O_3 4.0–5.0; TiO_2 0.3–1.0; CaF_2 0.5–2.4; MnO_2 1.0–2.0; MgO 0.1–1.0; CeO_2 0.4–0.5; CoO 0.01–0.03; V_2O_5 0.02–0.03; SrO 0.01–0.04; Cu_2O 0.01; MoO_3 0.01–0.02; La_2O_3 0.01–0.02; and ZrO_2 filler at 5 mass parts per 100 mass parts of frit. Histological analysis 30 days post-operation showed lamellar bone tissue formation around the implant area, with trabeculae aligned along the developed material's surface. Accelerated apatite-like layer formation on the surface of developed material, along with bactericidal activity against *E. coli* and *Staphylococcus aureus*, enables faster bone regeneration and significantly shortens rehabilitation periods after prosthetic surgeries.[24] However, the insufficient fracture toughness of the developed material remains a significant limitation for its application in load-bearing areas of long bones, particularly in the lower limbs (Table 1).

Table 1. Comparative Characteristics of Foreign and Domestic Bioactive Glass-Ceramic Materials

Name	Component Content, mass% Crystalline Phases	Manufacturing Method	Mechanical Properties	Country, Author, Year
1	2	3	4	5
Ceravital	CaO 30–35, P_2O_5 19–50, SiO_2 40–50; impurities: Na_2O 5–10, K_2O 0.5–3.0, MgO 2.5–5; Crystalline phase: apatite	Melt casting, thermal treatment	σ_{bend} up to 150 MPa	Germany, H. Bremer *et al*., 1973
Cerabone	CaO 44.7, P_2O_5 6.2, SiO_2 34; impurities: MgO 4.6, CaF_2 0.5; Crystalline phases: apatite, wollastonite	Glass powder sintering	σ_{bend} = 178 MPa, σ_{bend} (in nitrogen) = 215 MPa, $\sigma_{compressive}$ = 1060 MPa, E = 117 GPa	Japan, T. Kokubo *et al*., 1986
Biovitre	Na_2O 3–8, MgO 2–21, CaO 10–34, Al_2O_3 8–15, SiO_2 19–54; impurities: P_2O_5 2–10, F_2 3–23; Crystalline phases: fluorophlogopite, apatite	Melt casting, thermal treatment	K_{IC} = 2.0 MPa·$m^{1/2}$, σ_{bend} = 140–180 MPa, K_{IC} = 2.1 MPa·$m^{1/2}$ machinable E = 70–88 GPa	Germany, W. Vogel *et al*., 1983
Bioactive Glass-Ceramic (BS)	SiO_2 45–50; Al_2O_3 0–5; Na_2O 5–15; CaO 15–20; P_2O_5 5–10; B_2O_3 0–5; TiO_2 0–5	Glass powder sintering	σ_{bend} = 120 MPa, K_{IC} = 2.22 MPa·$m^{1/2}$, $\sigma_{compressive}$ = 400 MPa, HV = 4000 MPa	Ukraine, O. Savvova *et al*., 2012
Bioactive Glass-Ceramic (CF)	SiO_2 47–50; Al_2O_3 0–5; Na_2O 10; CaO 15–20; P_2O_5 5–10; B_2O_3 0–5; ZnO 5–8	Glass powder sintering	σ_n = 100 MPa, K_{IC} = 1.48 MPa·$m^{1/2}$, $\sigma_{compressive}$ = 400 MPa, HV = 4800 MPa	Ukraine, O. Savvova *et al*., 2014

Continuation of Table 1.

1	2	3	4	5
Reinforced Apatite Glass-Ceramic (RAGC)	SiO_2 47–50; Al_2O_3 2–3; Li_2O 2–4.5; Na_2O 3.5–6; K_2O 4; ZrO_2 0.5–1; P_2O_5 9–10; CaO 15–17; ZnO 1–3; B_2O_3 4–5; TiO_2 0.3–1; CaF_2 0.5–2.4; MnO_2 1–2; MgO 0.1–1; CeO_2 0.4–0.5; CoO 0.01–0.03; V_2O_5 0.02–0.03; SrO 0.01–0.04; Cu_2O 0.01; MoO_3 0.01–0.02; La_2O_3 0.01–0.02; with ZrO_2 filler – 5 parts per 100 parts frit. Crystalline phase: apatite	Glass powder sintering	σ_n = 160 MPa, K_{IC} = 2.8 MPa·$m^{1/2}$, $\sigma_{compressive}$ = 400 MPa, HV = 3800 MPa	Ukraine, O. Savvova *et al.*, 2020

Addressing this challenge involves the development of glass-ceramic materials that simultaneously contain crystalline phases with high biological activity (apatite, carbonate apatite, fluorapatite) and mechanical strength (*e.g.*, diopside, anorthite, spodumene, *etc.*).[25] Another novel approach in the development of high-strength glass-ceramic materials involves surface modification to enhance bioactivity and strengthen the surface through crack healing and surface crystallization processes.[26,27] These strategies underline the relevance of developing domestic high-strength calcium phosphate glass-ceramic materials for the restoration of long bone defects.

2. Experimental

2.1. Materials

The core idea of this work is to develop high-strength glass-ceramic materials based on calcium phosphate silicate glasses for the controlled restoration of large metaphyseal and diaphyseal defects in long bones.

The development of bone substitute materials is based on fundamental principles of biomimetics – reproducing the functionality of the target organ by mimicking the structure and phase composition of biological tissue. The structure of long tubular bones comprises the epiphysis and metaphysis, which are predominantly formed by trabecular bone, and the diaphysis, which consists of compact bone (Fig. 1).[28] Moreover, long tubular bones – such as the femur, tibia, and fibula; as well as the humerus, ulna, and radius – are subjected to different mechanical loads (Table 2).[29]

These materials serve as the basis for creating scaffolds – porous, bioactive, nanostructured glass-ceramic materials with controlled architecture. A fundamentally new approach in the development and further refinement of scaffolds for bone tissue engineering is the concept of using bioactive glass-ceramic materials as osteoconductive matrix-carriers. These materials possess tunable mechanical properties, rapidly integrate with bone tissue (within 1–3 months), are capable of withstanding dynamic and static loads over large bone regions, and ensure effective osteoconduction.

The primary challenge in scaffold design is to simultaneously achieve high mechanical strength of the biomaterial and its rapid integration with native bone. The complexity of this task lies in a scientific paradox: achieving glass materials that exhibit both high structural strength and high biological activity, the latter of which is largely determined by material resorption.

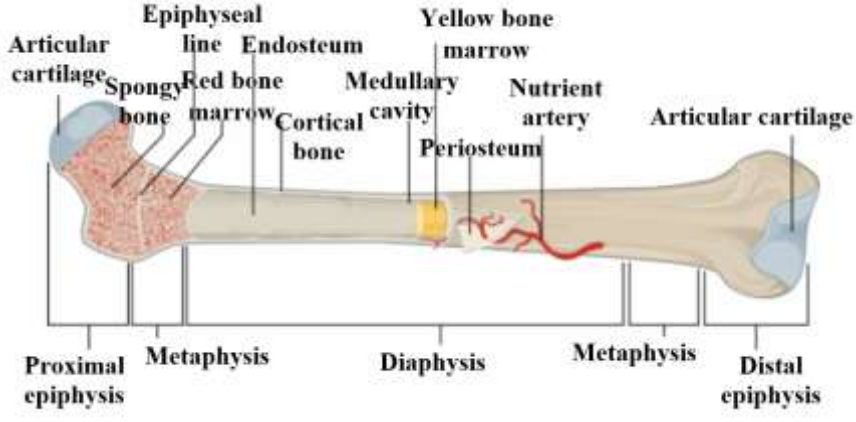

Fig. 1. Structure of a long tubular bone

Table 2. Mechanical Properties of Long Tubular Bones

Bone Tissue	Loading Direction	Elastic Modulus GPa)	Tensile Strength (MPa)	Compressive Strength (MPa)
Femur	Longitudinal	17.2	121.0	167.0
Tibia	Longitudinal	18.1	140.0	159.0
Fibula	Longitudinal	18.6	146.0	129.0
Humerus	Longitudinal	17.2	130.0	132.0
Radius	Longitudinal	18.6	149.0	114.0
Ulna	Longitudinal	18.0	148.0	117.0

It is well known that the incorporation of alkali metals significantly enhances the solubility of glass materials and may detrimentally affect their mechanical strength. On the other hand, for proper bone formation, it is essential to trigger the bioactivity mechanism of glass materials, which involves gradual resorption of the material and the formation of an apatite-like layer on the implant surface, followed by comprehensive mineralization. It should be noted that the rate of bone tissue formation at the site of biomaterial replacement should match the bone regeneration rate of the host organism. Otherwise, in cases of delayed integration – as observed with hydroxyapatite (HA) – the healing process may extend over 1–2 years. Conversely, accelerated degradation may provoke immune responses due to the excessive release of ionic elements, leading to inflammation, rejection, and possible mechanical failure of the material.

Taking into account the principles of biomimetics and biomechanics of long tubular bones, the following key requirements for glass-ceramic materials have been formulated to ensure accelerated bone-biomaterial integration:

– Formation of a nanostructured glass texture through phase separation and subsequent crystallization under low-temperature thermal treatment conditions;

– Crystallization of bioactive phases (hydroxyapatite, carbonate hydroxyapatite) alongside chemically durable phases (anorthite, diopside, lithium disilicate, spodumene) in an amount exceeding 50 vol.%, forming an interconnected structural network;

– Achievement of biological activity through regulated resorption of the glass matrix and crystalline phases;

– Assurance of non-toxicity by incorporating metal cations into the glass matrix structure;

– Modulation of structural, enzymatic, metabolic, and anti-inflammatory properties of bone tissue via microelemental modification.

These requirements, firstly, will ensure the high strength of glass-ceramic materials, making them suitable for use in both trabecular and cortical bone replacement. Secondly, they will accelerate mineralization by activating processes involving microelements within the organism, which directly or indirectly influence bone tissue formation (Table 3).

Therefore, the development of high-strength bioactive glass-ceramic materials modified with heavy metal cations for long bone defect reconstruction constitutes a critical scientific and applied task that necessitates comprehensive investigation.

2.2. Methods

X-ray diffraction (XRD) analysis was conducted using a DRON-UM1 diffractometer with Cu-Kα radiation and a Ni-selective absorption filter. Diffracted radiation was registered with a scintillation detector.

Phase identification (qualitative phase analysis) was performed using the Crystallography Open Database (COD). Quantitative phase analysis and the determination of structural parameters of the identified phases were carried out using the Rietveld refinement method [1], with the MAUD software package. It should be noted that in certain cases, specific lattice parameters of some phases were not refined (held fixed) due to their low symmetry or minor content in the sample. For samples containing both crystalline and amorphous phases, the degree of crystallinity (approximately corresponding to the volume fraction of the crystalline phase) was calculated using the formula:

$$X_c = {}^{I_c}/_{(I_c + I_a)} \cdot 100\% \qquad (1)$$

where X_c is the degree of crystallinity; I_c is the total integral intensity of diffraction peaks, I_a is the integral intensity of the diffraction halo.

The crystallization potential of the experimental glasses under thermal treatment was studied using gradient thermal analysis (gradient furnace), petrographic analysis (NU-2E polarization microscope), and dilatometric analysis (Q-1500D derivatograph, Paulik-Paulik-Erdey system).

Fracture toughness (KIC) was measured by indenting with a Vickers pyramid under a 5000 g load, based on 10 measurements using a TMV-1000 device. Compressive strength was determined by placing the test sample between two plates and applying a slowly

increasing all-around force until it failed. Bending strength was determined by testing material samples for bending until they broke. Coefficient of Thermal Expansion (CTE) was determined by the relative elongation of materials Δl/l, % upon heating ($(\Delta t_I – t_F)$ on a vertical quartz dilatometer DKV-5A. The CTE values were calculated for each temperature interval. The experimental glasses of the OSM series were melted under identical conditions at temperatures of 1400–1450 °C in corundum crucibles.

Glass-ceramic materials based on these experimental glasses were obtained from powders ground to a residue of no more than 5% on sieve No. 008. The powders were then shaped by semi-dry isostatic pressing (P = 35–40 MPa, temporary binder: 4% xanthan gum solution) into cylindrical specimens with a diameter of 4 mm and a height of 10 mm.

Calcium phosphate silicate glasses (OS series) were previously developed with the following components introduced into their composition:[30,31]

– Glass formers: Al_2O_3 and B_2O_3, used to stabilize the silica-oxygen framework by maintaining a $\Psi_{B/Al} > 1$ ratio, thereby promoting the formation of $[BO_4]$ and $[AlO_4]$ tetrahedra in the glass structure;

– Modifiers: Na_2O, K_2O, Li_2O, MgO, and SrO to regulate the resorption rate of the glasses;

– Phase formers: with a CaO/P_2O_5 ratio of 1.67–1.7 and a SiO_2/Li_2O ratio of 4 to promote the crystallization of hydroxyapatite and lithium disilicate;

– Crystallization catalysts: ZrO_2, TiO_2, ZnO, CeO_2, CaF_2;

– Proliferation activator: Nb_2O_3, to enhance preosteoblast proliferation;

– Bactericidal agent: Ga_2O_3

The OS series compositions were modified (OSM series) to accelerate bone tissue formation by increasing reactivity – achieved by reducing SiO_2 and Al_2O_3 contents by 2 mass % and increasing the concentration of $Nb_2O_3 + Ga_2O_3$ up to 1–2 mass %. Additionally, new bioactive components acting as bone tissue cofactors and mineralization agents were introduced, including V_2O_5, CoO, MoO_3, MnO_2, FeO, La_2O_3, and Ta_2O_5 (Fig. 2, Table 3).

The selection of lanthanide oxides and oxides of tantalum and niobium was based on their ability to promote adhesion and proliferation of preosteoblasts and mesenchymal stem cells (MSCs). Meanwhile, lanthanum and gallium oxides provided anti-inflammatory and antiseptic effects.

A calculated crystallization coefficient $K_{cr} > 3.5$ indicates that the total content of modifier oxides in the melt is sufficient for the formation of structurally ordered sybotactic clusters that serve as nucleation sites for crystalline phases. A transparency coefficient $K_{transp} > 2.1$ suggests favorable conditions for nucleation during cooling and crystal growth during thermal treatment.

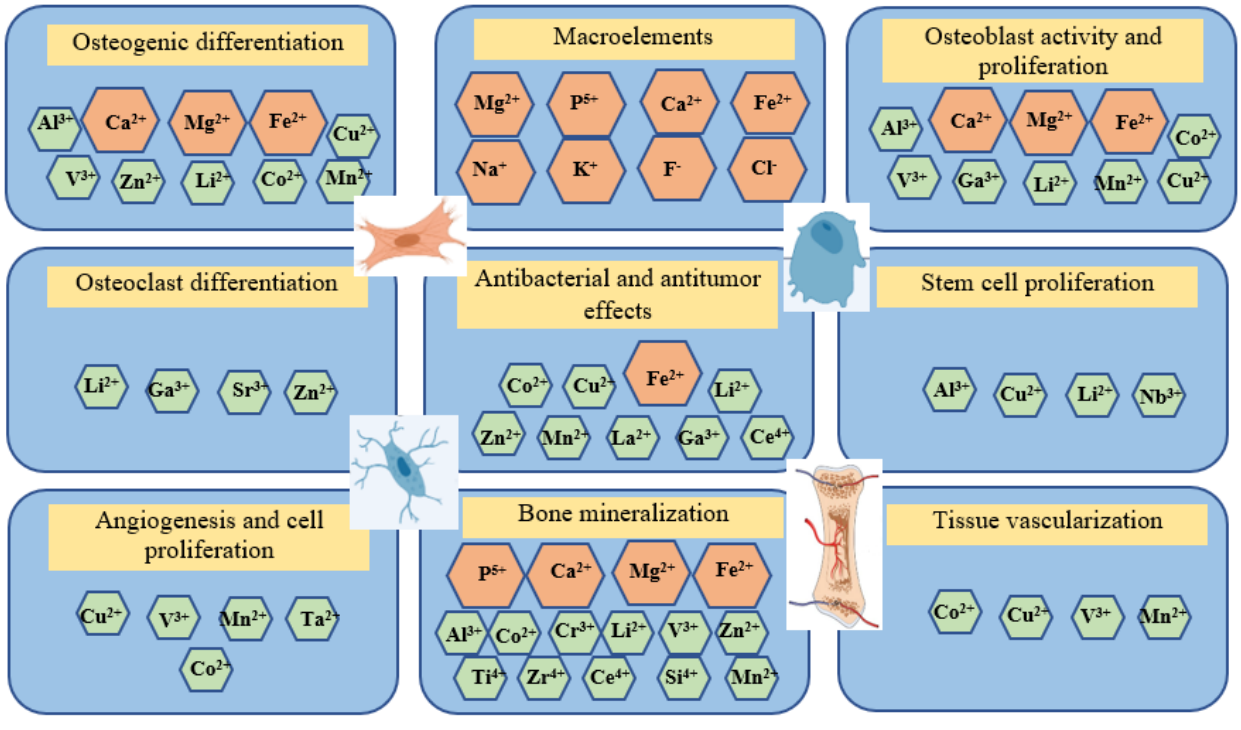

Fig.2. Influence of metal ions on various processes involved in bone tissue regeneration

Table 3. Differences in the chemical composition of experimental glasses

Components	OSM Glass Composition Number										
	1	2	3	4	5	6	7	8	9	10	11
Σ (SiO_2 + Li_2O)	65.75	57.0	57.0	62.0	58.0	60.75	63.0	59.5	57.0	62.0	65.0
Σ (Al_2O_3, B_2O_3)	5.0	4.0	3.0	3.0	3.0	4.0	3.5	3.0	5.0	5.2	4.2
Σ (Nb_2O_3+Ga_2O_3)	2.0	1.0	1.0	2.0	1.0	2.0	1.5	1.5	1.5	0.2	0.2
Σ (CaO, P_2O_5 + CaF_2+ Ta_2O_5)	21.95	24.5	33.9	28.0	29.5	23.25	24.5	29.0	26.2	27.1	25.1
Σ (K_2O+Na_2O)	0.8	2.0	0.6	0.5	1.0	1.5	1.0	0.5	1.8	2.0	2.0
Σ (ZnO + SrO+ MgO)	2.0	6.0	2.0	2.0	3.0	4.0	3.0	3.0	4.0	2.2	2.2
Σ (TiO_2 + ZrO_2 + SnO_2 + CeO_2)	2.0	5.0	2.0	2.0	4.0	4.0	3.0	3.0	4.0	0.8	0.8
Σ (V_2O_5, CoO, MoO_3, MnO_2, FeO, La_2O_3)	0.5	0.5	0.5	0.5	0.5	0.5	0.5	0.5	0.5	0.5	0.5
f_{Si}	0.29	0.26	0.26	0.28	0.27	0.28	0.28	0.27	0.27	0.27	0.28
$\Psi_{Al/B}$	7.94	9.21	14.11	12.95	13.67	8.63	10.12	13.05	8.46	9.21	8.63
K_{transp}	2.69	2.9	2.87	2.80	2.88	2.81	2.79	2.85	2.76	2.81	2.7
K_{cr}	13.8	9.21	17.46	19.27	12.62	11.38	14.22	13.86	11.91	14.99	15.54

3. Results and Discussion

The optimal selection of glass-ceramic materials for bone tissue replacement is primarily determined by their phase composition and structure, particularly the content and ratio of crystalline phases to the glassy matrix. A critical factor in the formation of a glass-ceramic structure is the sequence of crystalline phase emergence and the temperatures at which structural transformations occur.

Differential thermal analysis (DTA) provides insight into the characteristic temperatures associated with the structural evolution of the investigated glass materials (Fig. 3):

1. Temperature ranges of 130–170°C correspond to the removal of bound water, and 330–400°C to the release of residual stresses.

2. The glass transition interval (T_g–T_f) determines the temperatures of phase separation, structural clustering, and nucleation of crystals. These processes correlate with specific peaks observed on the viscosity curves of the test glasses. For glasses OSM-2, OSM-7, OSM-10, and OSM-11, this interval is narrow and shifted toward lower temperatures, specifically 550–650°C and 500–550°C, respectively (Fig. 3). Such low-temperature nucleation is important for the formation of a high-strength structure, as the first crystalline phases to form are metastable and chemically similar to the parent glass matrix, resulting in strong interfacial bonding. OSM-5 glass, on the other hand, exhibits a broad glass transition interval (600–800 °C), indicating intensive crystal growth, which is supported by a sharp increase in viscosity at 600°C to $\eta = 10^{9.2}$ Pa·s. The proximity of the first exothermic peak to the T_g–T_f range confirms that crystallization in all tested glasses occurs at high viscosities near the softening point, implying that glass-ceramization can proceed without deformation of the samples. A distinguishing feature of OSM-7 is the presence of a minor exothermic effect near the softening temperature T_f, which may suggest phase separation occurring around 600 °C, where viscosity reaches $\eta = 10^{8.5}$ Pa·s.

3. The crystallization interval of the experimental glasses is relatively broad and comprises two stages: 650–800°C: active crystal growth; 800–900°C: development of the glass-ceramic structure. A notable feature of the calcium-phosphate-silicate glass samples is the absence of sharp exothermic peaks, which usually indicate intensive formation of crystalline phases in a narrow temperature window. This is attributed to the fact that the glass already contains some pre-formed crystalline phase after melting. The narrow exothermic peaks observed in glasses OSM-2 and OSM-7 may suggest the formation of a fine-dispersed crystalline structure, which enhances the mechanical strength of the material.

The results of gradient-thermal analysis (Fig. 4) and petrographic analysis (Table 4) confirm the occurrence of intensive crystallization processes in the tested glasses, corresponding to the identified nucleation and crystal growth temperature intervals. In glasses OSM-3, OSM-4, OSM-5, and OSM-8, which are rich in phase-forming components (ΣCaO, P_2O_5, CaF_2), crystallization is significantly enhanced in the temperature region of 800–900°C, corresponding to the growth of hydroxyapatite (HAP) crystals.

A reduction in phase-forming oxides (ΣCaO, P_2O_5, CaF_2) in glasses OSM-1, OSM-2, OSM-7, OSM-9, OSM-10, and OSM-11 shifts the crystallization to a lower temperature region (650–700°C), favoring the formation of lithium metasilicate and eucryptite phases. This low-

temperature crystallization is facilitated by fluctuation-driven structural rearrangements in systems with low energy barriers, which is optimal for the synthesis of high-strength glass-ceramics in a shortened timeframe.

Full crystallization of the test glasses is achievable only in the presence of crystallization catalysts. A comparison between glasses OSM-1 to OSM-9, containing catalysts like TiO_2, ZrO_2, and SnO_2, and those containing ZnO and CeO_2 demonstrates that the latter significantly lowers the crystallization temperature range. Consequently, in glasses OSM-10 and OSM-11, partial melting is observed in the 800–900°C region. This behavior is linked to the high content of low-viscosity glassy phase rich in alkali components, which may lead to a critical increase in the resorption of the investigated materials and exclude the possibility of creating high-strength glass materials based on them for the replacement of long bones.

The introduction of active additives such as V_2O_5, CoO, MoO_3, MnO_2, FeO, and La_2O_3 into the modified OSM glasses slightly enhances their crystallization ability compared to the original OS glass compositions[30]. Petrographic investigations of thermally treated glasses (6 hours in a gradient furnace) reveal the formation of primary crystalline phases: hydroxyapatite phase (31.0–62.0 vol. %), β-spodumene (16.8–22.1 vol. %), β-eucryptite (5.0–21.9 vol. %), lithium phosphate (2.0–5.9 vol. %), lithium disilicate (4.2–6.9 vol. %), and diopside (4.0–6.6 vol. %). The developed glass compositions demonstrate a balanced phase composition, combining bioactive phases with high-strength thermally stable lithium aluminosilicates, which help prevent crack formation during cooling and ensure defect-free material consolidation. Moreover, the presence of lithium-containing crystalline phases not only enhances mechanical reinforcement but also provides biological advantages due to the presence of lithium cations, known to promote regeneration of bone, cartilage, and dentin, exhibit anti-inflammatory, antibacterial, and anticancer properties, accelerate wound healing and limit infection spread. A significant structural distinction is observed between the developed glass-ceramics: OSM-3, OSM-4, OSM-5, OSM-8, and OSM-9 contain large crystals (1–3 μm) (Table 5), resulting from high-temperature crystallization of HAP, whereas OSM-2, OSM-6, OSM-7, OSM-10, and OSM-11 exhibit fine-grained crystallization, which is a key factor for strength enhancement under mechanical loading.

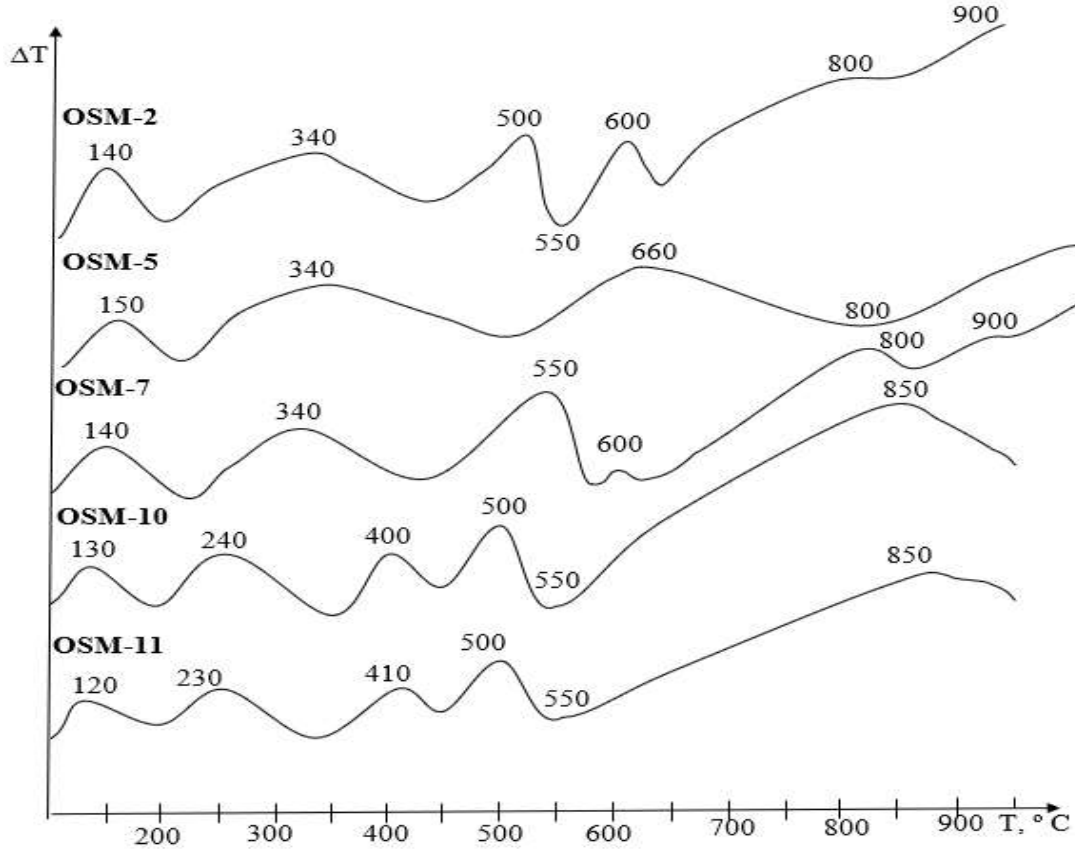

Fig. 3. Thermograms of experimental glasses

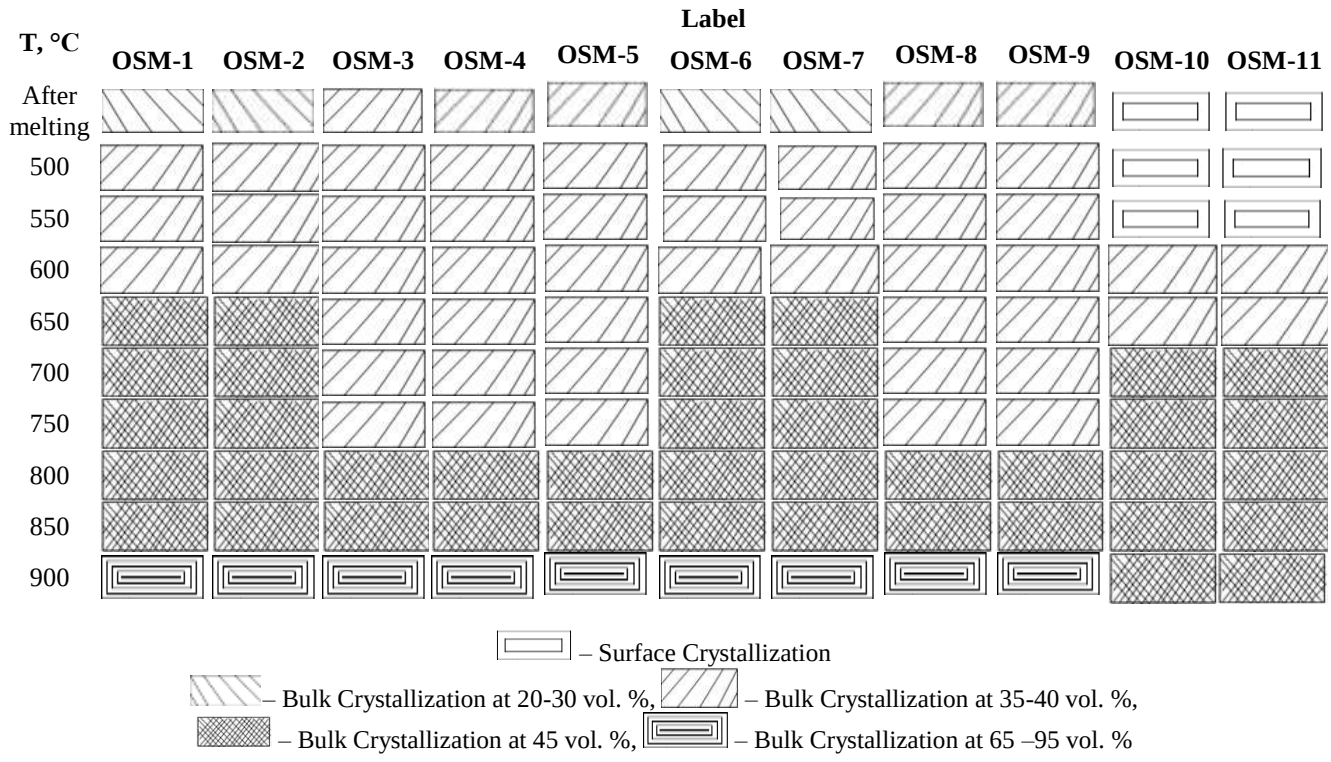

Fig.4. Crystallization capacity of experimental glasses from the OSM series during heat treatment by the gradient-thermal analysis method and the resulting crystalline phase content

Table 4. Types and contents of crystalline phases and their unit cell parameters in the developed OSM series glass-ceramic materials after three-stage heat treatment.

Glass-ceramic Material	Crystalline Phases	Phase Content (vol. %)	Unit Cell Parameters
1	2	3	4
OSM-2	Spodumene-II	22.1	a = 7.522; c = 9.108
	Hydroxyapatite	58.4	a = 9.379; c = 6.894
	Lithium phosphate	5.4	a = 6.128; b = 10.479; c = 4.933
	Diopside	4.1	a = 9.753; b = 8.931; c = 5.263; β = 106.13°
	β-Eucryptite	5	a = 10.499; c = 11.114
	Glass phase	5	
OSM-7	Spodumene-II	21.8	a = 7.533; c = 9.128
	Hydroxyapatite	58.5	a = 9.383; c = 6.911
	Lithium phosphate	5.3	a = 6.144; b = 10.506; c = 4.946
	Diopside	2.1	a = 9.75; b = 8.92; c = 5.25; β = 105.94°
	β-Eucryptite	7.3	a = 10.497; c = 11.075
	Glass phase	5	
OSM-10	Spodumene-II	16.8	a = 7.547; c = 9.129
	Hydroxyapatite	36.0	a = 9.408; c = 6.953
	Lithium phosphate	5.9	a = 6.144; b = 10.506; c = 4.946
	Diopside	4.3	a = 9.74; b = 8.90; c = 5.24; β = 105.72°
	β-Eucryptite	21.9	a = 10.499; c = 11.114
	Li_2Si2O_5	5.1	a = 9.432; b = 5.395; c = 4.675
	Glass phase	10	–

Continuation of Table 4.

1	2	3	4
OSM-11	Spodumene-II	19.1	a = 7.532; c = 9.129
	Hydroxyapatite	46.2	a = 9.408; c = 6.953
	Lithium phosphate	5.9	a = 6.144; b = 10.506; c = 4.946
	Diopside	6.6	a = 9.74; b = 8.90; c = 5.24; β = 105.72°
	β-Eucryptite	5.3	a = 10.499; c = 11.114
	Li_2Si2O_5	6.9	a = 9.432; b = 5.395; c = 4.675
	Glass phase	10	–

Table 5. Size of crystals in the structure of the research materials

Crystal size, μm	Glass-ceramic materials										
	OSM-1	OSM-2	OSM-3	OSM-4	OSM-5	OSM-6	OSM-7	OSM-8	OSM-9	OSM-10	OSM-11
	< 1	< 1	1-3	1-3	1-3	< 1	< 1	1-3	1-3	< 1	< 1

The research results enabled the selection of optimal heat treatment parameters for the glasses: Stage I – 550–650°C, Stage II – 800°C, Stage III – 900°C, as well as a short-term (30 minutes) treatment mode. These conditions allowed for the synthesis of experimental glass-ceramic materials with a defect-free structure. The developed high-strength bioactive glass-ceramic materials (GCMs), treated under the specified regime, are characterized by the presence of the bioactive hydroxyapatite phase (31.0–62.0 vol. %), β-spodumene (16.8–22.1 vol. %), β-eucryptite (5.0–21.9 vol. %), lithium phosphate (2.0–5.9 vol. %), lithium disilicate (4.2–6.9 vol. %), and diopside (4.0–6.6 vol. %). The priority of simultaneous synthesis of bioactive and high-strength thermally stable phases in the developed glass-ceramic materials is a key factor for their implementation in clinical practice for bone tissue replacement in load-bearing areas.

A comparative analysis of different types of bone tissue (Table 6),[32,33] along with the mechanical properties of long bones (Table 2), established that the developed glass-ceramic material OSM-7 corresponds to the mechanical properties of cortical bone and can be effectively used for bone tissue replacement. A notable feature of the developed material is its high fracture toughness, which is typically low for known glass-ceramics (Table 1), limiting their application in load-bearing bone segments and in the development of tissue-engineered constructs for replacing large sections of bone.

4. Conclusions

Based on an analysis of the challenges associated with bone tissue damage caused by osteoporosis, congenital defects, or trauma (including explosive injuries), there is a critical need to develop endoprostheses for the reconstruction of long bone defects. The use of biocompatible composite materials – scaffolds based on bioactive inorganic substances in combination with growth factors and natural polymers –has been identified as a promising approach for rapid bone regeneration and minimizing blood loss.

Bioactive glass compositions were developed based on the lithium-calcium-silico-phosphate system, incorporating the following components: glass-forming oxides: Al_2O_3, B_2O_3; modifiers: Na_2O, K_2O, MgO, SrO; ₚhase-forming oxides: CaO, P_2O_5, SiO_2, Li_2O; Crystallization catalysts: ZrO_2, TiO_2, ZnO, CeO_2, CaF_2; Preosteoblast and MSC proliferation activators: Nb_2O_3, Ta_2O_5; Bactericidal agents: La_2O_3, Ga_2O_3; Cofactors and mineralizers for bone tissue: V_2O_5, CoO, MoO_3, MnO_2, FeO. Technological parameters were selected, and glass-ceramic material compositions were synthesized featuring the formation of a bulk crystallized structure through a three-stage process: Nucleation via phase separation (550–650°C, 15 min); Nanostructuring and formation of solid solutions based on calcium and lithium phosphates, lithium metasilicate, and β-eucryptite, followed by recrystallization into β-spodumene (650–850°C, 10 min); Crystallization and devitrification of the glass with a crystalline phase content of 90–95 vol. % (850–900°C, 5 min).

The developed high-strength bioactive glass-ceramic materials, which simultaneously exhibit bioactivity, osteoinductivity, bactericidal properties, mechanical strength, and thermal strength, are promising candidates for regenerative medicine, particularly in emergency and crisis scenarios.

Table 6. Comparative characteristics of the mechanical properties of bone tissue, Bioglass 45S5, and the developed OSM series glass-ceramic materials.

Material property	Trabecular bone	Cortical bone	Bioglass 45S5	OSM-2	OSM-7	OSM-10	OSM-11
Compressive strength (MPa)	0.1–16	130–200	500	570±10	650±10	550±10	620±10
Bending strength (MPa)	n.a.	50–151	42	400±10	450±10	350±10	400±10
Fracture toughness (MPa $m^{1/2}$)	n.a.	2–12	0.9	5.1±0.5	6.1±0.5	4.5±0.5	5.0±0.5
Coefficient of Thermal Expansion α 10^{-7}°C^{-1}	n.a.	275	150	79.2	70.5	40.5	60.3

References

[1] Li, M.; Yu, B.; Yang, H; He, H. Trends and Hotspots in Research on Osteoporosis and Nutrition from 2004 to 2024: A Bibliometric Analysis. *J. Health Popul. Nutr.* **2024**, *43*, 204. https://doi.org/10.1186/s41043-024-00690-5

[2] Anish, R.J.; Nair, A. Osteoporosis Management-Current and Future Perspectives - A Systemic Review. *J. Orthop*. **2024**, *2*, 101–113. https://doi.org/10.1016/j.jor.2024.03.002

[3] Dussault, M.C.; Smith, M.; Osselton, D. Blast Injury and the Human Skeleton: An Important Emerging Aspect of Conflict-Related Trauma. *J. Forensic Sci*. **2014**, *59*, 606–612. https://doi.org/10.1111/1556-4029.12361

[4] Kluger, Y.; Bahouth, H.; Harbi, A. Blast Injuries: Tips, Evaluation, and Management. *In Emergency Medicine.Trauma and Disaster Management*; Pikoulis, E.; Doucet, J. (eds); Springer, Cham. 2021; pp 289–297. https://doi.org/10.1007/978-3-030-34116-9_21

[5] Burianov, O.; Kvasha, V.; Sobolevskiy, Y.; Yarmoliuk, Y.; Klapchuk, Y.; Los, D.; Kuprii, V.; Kolov, G. Methodological Principles of Diagnosis Verification and Treatment Tactics Determination in Combat Limb Injuries with Bone Defects. *Orthopaedics Traumatology and Prosthetics* **2024**, *4*, 5–13. https://doi.org/10.15674/0030-5987202345-13

[6] Lurin, I.; Burianov, O.; Yarmolyuk, Y.; Klapchuk, Y.; Derkach, S.; Gorobeiko, M.; Dinets, A. Management of Severe Defects of Humerus in Combat Patients Injured in Russo-Ukrainian War. *Injury* **2024**, *55*, 111280. https://doi.org/10.1016/j.injury.2023.111280

[7] Hrytsai, M.P.; Kolov, H.B.; Sabadosh, V.I.; Vyderko, R.V.; Polovyi, A.S.; Hutsailiuk, V.I. Osnovni khirurhichni metody zamishchennia krytychnykh kistkovykh defektiv velykohomilkovoi kistky. (Ohliad literatury). *TERRA ORTHOPAEDICA* **2024**, *2*, 45–53. https://doi.org/10.37647/2786-7595-2024-121-2-45-53

[8] Yu, H.; Liu, H.; Shen, Y.; Ao, Q. Synthetic Biodegradable Polymer Materials in the Repair of Tumor-Associated Bone Defects. *Front. Bioeng. Biotechnol*. **2023**, *16*, 1096525. https://doi.org/10.3389/fbioe.2023.1096525

[9] Elshazly, N.; Eid Nasr, F.; Hamdy, A.; Saied, S.; Elshazly, M. Advances in Clinical Applications of Bioceramics in the New Regenerative Medicine Era. *World Journal of Clinical Cases* **2024**, *16*, 1863–1869. https://doi.org/10.12998/wjcc.v12.i11.1863

[10] Zhang, M.; Matinlinna, J.P.; Tsoi, J.K.H; Liu, W; Cui, X.; Lu, W.W.; Pan, H. Recent Developments in Biomaterials for Long-Bone Segmental Defect Reconstruction: A Narrative Overview. *J. Orthop. Translat*. **2019**, **22**, 26–33. https://doi.org/10.1016/j.jot.2019.09.005

[11] Barreto, M.E.V.; Medeiros, R.P.; Shearer, A.; Mauro, J.C. Gelatin and Bioactive Glass Composites for Tissue Engineering: A Review. *J. Funct. Biomater.* **2023**, *14*, 23. https://doi.org/10.3390/jfb14010023

[12] Guo, A. X.Y.; Cheng, L.; Zhan, S.; Zhang, S.; Xiong, W.; Wang, Z.; Wang, G.; Cao, S. C. Biomedical Applications of the Powder-Based 3D Printed Titanium Alloys: A Review. *J. Mater. Sci. Technol*. **2022**, *125*, 252–264. https://doi.org/10.1016/j.jmst.2021.11.084

[13] Correa-Araujo, L.; Lara Bertrand, A.; Silva-Cote, I. Tissue Engineering Scaffolds: The Importance of Collagen. In *Cell and Molecular Biology*; Mary C. Maj, M.C.; and Felicia Ikolo, F., Eds.; 2024. https://doi.org/10.5772/intechopen.1004077

[14] Diedkova, K.; Pogrebnjak, A.D.; Kyrylenko, S.; Smyrnova, K.; Buranich, V.V.; Horodek, P.; Zukowski, P.; Koltunowicz, T.N.; Galaszkiewicz, P.; Makashina, K.; *et al*. Polycaprolactone-MXene Nanofibrous Scaffolds for Tissue Engineering. *ACS Appl. Mater. Interfaces.* **2023**, *15*, 14033–14047. https://doi.org/10.1021/acsami.2c22780

[15] Samokhin, Y.; Varava, Y.; Diedkova, K.; Yanko, I.; Husak, Y.; Radwan-Pragłowska, J.; Pogorielova, O.; Janus, Ł.; Pogorielov, M.; Korniienko, V. Fabrication and Characterization of Electrospun Chitosan/Polylactic Acid (CH/PLA) Nanofiber Scaffolds for Biomedical Application. *J. Funct. Biomater*. **2023**, *14*, 414. https://doi.org/10.3390/jfb14080414

[16] Qin, H.; Wei, Y.; Han, J.; Jiang X.; Yang, X.; Wu, Y.; Gou, Z.; Chen, L. 3D printed Bioceramic Scaffolds: Adjusting Pore Dimension is Beneficial for Mandibular Bone Defects Repair. *J. Tissue Eng. Regen. Med*. **2022**, *16*, 409–421. https://doi.org/10.1002/term.3287

[17] Kamboj, N.; Ressler, A.; Hussainova, I. Bioactive Ceramic Scaffolds for Bone Tissue Engineering by Powder Bed Selective Laser Processing: A Review. *Materials* **2021**, *14*, 5338. https://doi.org/10.3390/ma14185338

[18] Kędzia, O.; Lubas, M.; Dudek, A. Glass and Glass-Ceramic Porous Materials for Biomedical Applications. *System Safety: Human - Technical Facility - Environment*. **2023**, *5*, 302–310. https://doi.org/10.2478/czoto-2023-0033

[19] Aalto-Setälä, L.; Siekkinen, M.; Lindfors, N.; Hupa, L. Dissolution of Glass–Ceramic Scaffolds of Bioactive Glasses 45S5 and S53P4. *Biomedical Materials & Devices* **2022**, *1*, 871–88. https://doi.org/10.1007/s44174-022-00059-4

[20] Workie, A.B.; Shih, S.J. A study of Bioactive Glass-Ceramic's Mechanical Properties, Apatite Formation, and Medical Applications. *RSC Adv*. **2022**, *16*, 23143–23152. https://doi.org/10.1039/d2ra03235j

[21] Da Fonte Ferreira, J. M.; Goel A. Bioactive Glass Composition, its Applications and Respective Preparation Methods. US 20140193499A1, April 5, 2012.
[22] Savvova, O.V.; Shimon, V.M.; Babich, O.V.; Fesenko, O.I. Development of Calcium Phosphate-Silicate Glass Ceramic Materials Resistant to Biochemical and Mechanical Destruction. *Funct. Mater*. **2020**, *27*, 767–773. https://doi.org/10.15407/FM27.04.767
[23] Savvova, O.; Shadrina, G.; Babich, O.; Fesenko, O. Investigation of Surface Free Energy of Glass-Ceramic Coatings on Titanium for Medical Purposes. *Chem. Chem. Technol*. **2015**, *9*, 349–354. https://doi.org/10.23939/chcht09.03.349
[24] Savvova, O. Biocide Apatite Glass-Ceramic Materials for Bone Endoprosthetics. *Chem. Chem. Technol*. **2013**, *7*, 109–112. https://doi.org/10.23939/chcht07.01.109
[25] Kirste, G.; Contreras Jaimes A.; de Pablos-Martín, A.; de Souza e Silva, J.M.; Massera, J.; Hill, R.G.; Brauer, D.S. Bioactive Glass–Ceramics Containing Fluorapatite, Xonotlite, Cuspidine and Wollastonite form Apatite Faster than their Corresponding Glasses. *Sci. Rep*. **2024**, *14*, 3997. https://doi.org/10.1038/s41598-024-54228-0
[26] Piatti E.; Miola M.; Verné E. Tailoring of Bioactive Glass and Glass-Ceramics Properties for *in vitro* and *in vivo* Response Optimization: A Review. *Biomater. Sci*. **2024**, *12*, 4546–4589. https://doi.org/10.1039/D3BM01574B
[27] Bartl, R.; Bartl, C. Structure and Architecture of Bone. In *The Osteoporosis Manual*; Springer, 2019; pp. 9–19. https://doi.org/10.1007/978-3-030-00731-7_2
[28] Cowan, P.T.; Launico, M.V.; Kahai, P. *Anatomy, Bones*; StatPearls Publishing, 2025.
[29] Guimarães, C.F.; Gasperini, L.; Marques, A.P.; Reis R. L. The Stiffness of Living Tissues and its Implications for Tissue Engineering. *Nat. Rev. Mater*. **2020**, *5*, 351–370. https://doi.org/10.1038/s41578-019-0169-1
[30] Savvova, O.V.; Fesenko, O.I.; Voronov, H.K.; Babich, O.V.; Bitiutska, V.V.; Smyrnova, Yu.O.; Hopko, A.O. Study of Mineralization of Lithium Calcium Phosphosilicate Glass Ceramics *in vivo* During Bone Tissue Regeneration. *Voprosy khimii i khimicheskoi tekhnologii* **2023**, *4*, 83–93. https://doi.org/10.32434/0321-4095-2023-149-4-83-93
[31] Savvova, O.; Fesenko, O.; Babich, O.; Voronov, H.; Smyrnova, Yu. Features of the Apatite-Like Layer Formation on the Surface of Bioactive Glass-Ceramic Materials *in vivo*. *Funct. Mater*. **2023**, *30*, 187–196. https://doi.org/10.15407/fm30.02.187
[32] Gerhardt, L.C.; Boccaccini, A.R. Bioactive Glass and Glass-Ceramic Scaffolds for Bone Tissue Engineering. *Materials (Basel)* **2010**, 6, 3867–3910. https://doi.org/10.3390/ma3073867
[33] Singh Ranu, H. Thermal Properties of Human Cortical Bone: An *in vitro* Study. *Engineering in Medicine* **1987**, *16*, 175–176. https://doi.org/10.1243/EMED_JOUR_1987_016_036_02

Received: June 01, 2025 / Revised: June 22, 2025 / Accepted: June 24, 2025

РОЗРОБКА ВИСОКОМІЦНИХ БІОАКТИВНИХ СКЛОКРИСТАЛІЧНИХ МАТЕРІАЛІВ ДЛЯ ЗАМІЩЕННЯ ДЕФЕКТІВ ДОВГИХ КІСТОК

Анотація. *Визначено нагальну потребу у відновленні опорно-рухового апарату людини, який пошкоджено внаслідок остеопорозу, вибухової травми та вроджених вад. Визначено потреби регенеративної медицини для відновлення кістки, які спрямовані на максимально можливе відновлення структури і функцій пошкоджених тканин. Встановлено необхідність розробки біоактивних матеріалів для заміщення дефектів довгих кісток через створення склокерамічних матеріалів з високою біологічною активністю та механічною міцністю.*

Розроблені високоміцні склокристалічні матеріали за швидкісної низькотемпературної термічної обробки з наявністю гідроксиапатиту, фосфату літію, сподумену, евкриптиту, діопсиду та дисилікату літію здатні витримувати значні механічні та термічні навантаження і є перспективними як основа для одержання замінників кісткової тканини елементів довгих кісток.

Ключові слова: *біоактивні склокристалічні матеріали, фазоутворення, гідроксиапатит, сподумен, механічні та термічні властивості.*